SUPPLEMENTARY METHODS

Western blot and immunoprecipitation

Whole cell lysates containing total protease inhibitor cocktail (Roche) of cultured mouse LECs treated as for the *in vitro* permeability assay were separated on 3-8% Tris-acetate gels (Thermo) and were subsequently transferred to PVDF membranes. After blocking in 5% fat-free milk in TBS + 0.1% Tween (TBS-T), membranes were blotted with goat anti-VE-cadherin (R&D AF1002) or rabbit anti-actin (Abcam ab8227) antibodies, followed by corresponding anti-goat (R&D HAF017) and anti-rabbit (Dako P0448) secondary antibodies conjugated to HRP. Signals were visualized with ECL Start substrate and ECL Hyperfilm (both GE Healthcare).
For immunoprecipitation, lysates additionally containing 1mM Na_3VO_4 and 5mM NaF were incubated with rabbit anti-ZO-1 (Thermo 61-7300) at 4°C O/N under rotation. Subsequently, Dynabeads conjugated with Protein-G (Thermo) were added and incubated for 20 min. Then, beads were washed and the bound proteins eluted according to the manufacturer's recommendations. Western Blot for phospho-serine was performed using 2% BSA for blocking, a primary mouse anti-phospho-serine antibody (Sigma P3430), and a sheep anti-mouse-HRP antibody (GE Healthcare NA931). After visualization, membranes were stripped and blotted for total ZO-1 using rabbit anti-ZO-1 and goat anti-rabbit-HRP (Dako P0448).

Blood vessel permeability in vivo

Blood vessel permeability was determined essentially as described before [1]. In brief, 0.05 nmol/g mouse weight of PEG40-IRDye800 were intravenously injected via the tail vein, and image series were taken on an IVIS Spectrum instrument (Perkin Elmer). Signal intensities in regions of interest covering the saphenous vein, the tumor, and the peri-tumoral area were determined using Living Image 4.0 (Perkin Elmer), and were used to calculate the vascular leakage rate as described [1].

SUPPLEMENTARY REFERENCES

[1] Proulx ST, Luciani P, Alitalo A, Mumprecht V, Christiansen AJ, Huggenberger R, Leroux JC, Detmar M. Non-invasive dynamic near-infrared imaging and quantification of vascular leakage in vivo. Angiogenesis 2013;16:525-40.

SUPPLEMENTARY FIGURES

Supplementary Figure S1

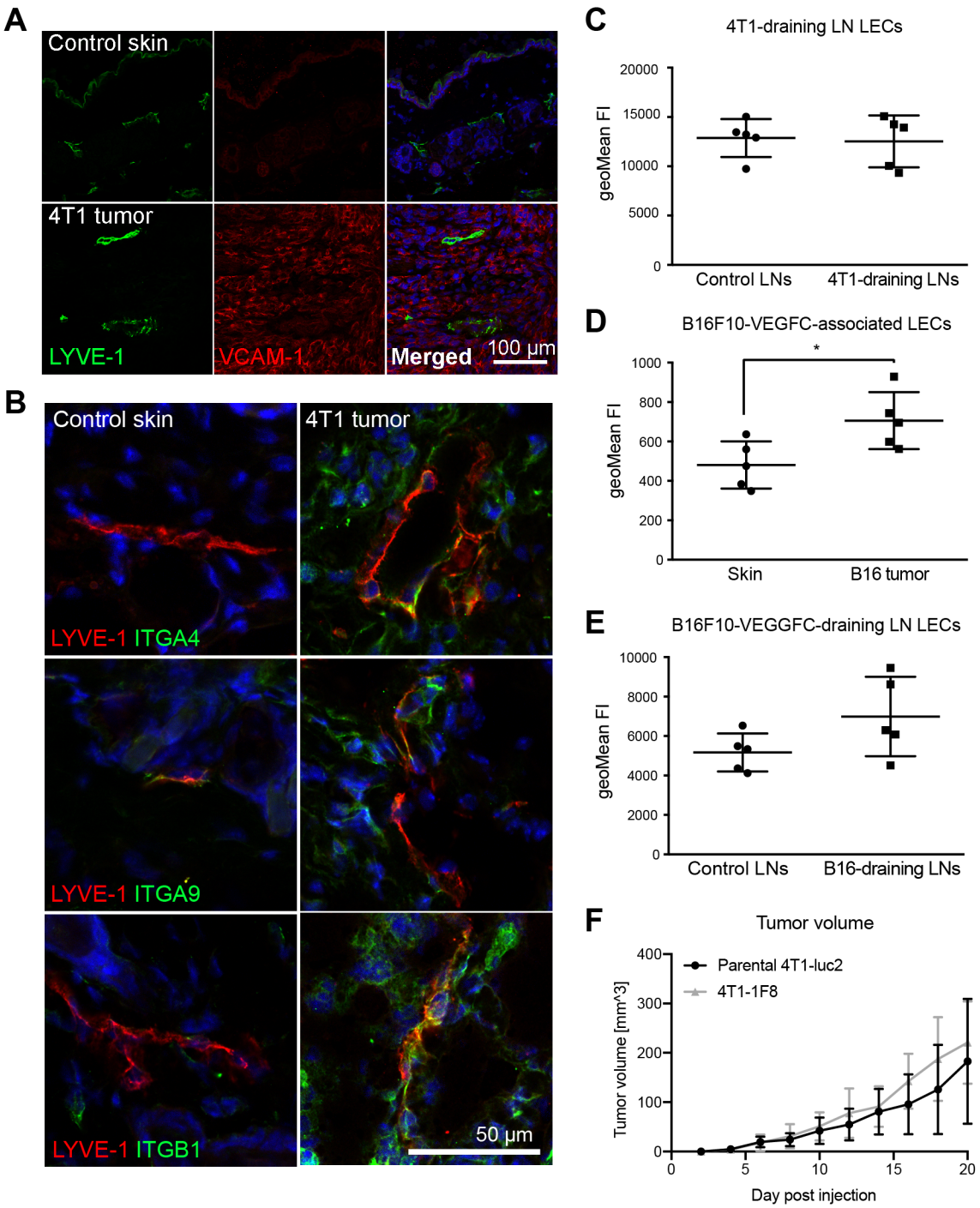

Figure S1: Expression of VCAM-1 in primary tumor and draining lymph node LECs. (A) Representative immunofluorescence staining for VCAM-1 (red) in control abdominal skin (Balb/c) and in 4T1 tumors. Lymphatic vessels are stained for LYVE-1 (green). (B) Example images of immunofluorescence stainings of integrin α4 (ITGA4, top panel), integrin α9 (ITGA9, middle panel), and integrin β1 (ITGB1, bottom panel) in control abdominal skin (Balb/c) and in 4T1 tumors. Lymphatic vessels are stained for LYVE-1 (red). (C) Flow cytometry analysis of VCAM-1 expression in 4T1 draining LN LECs (N = 5 mice / group).

(D) Flow cytometry analysis of VCAM-1 expression in B16F10-VEGFC associated LECs (N = 5 mice / group). (E) Flow cytometry analysis of VCAM-1 expression in B16F10-VEGFC draining LN LECs (N = 5 mice / group). (F) Tumor growth determined by caliper measurements in mice bearing parental 4T1-luc2 tumors and VCAM-1 knockout 4T1-1F8 tumors (N = 5 mice / group). (* $p < 0.05$).

Supplementary Figure S2

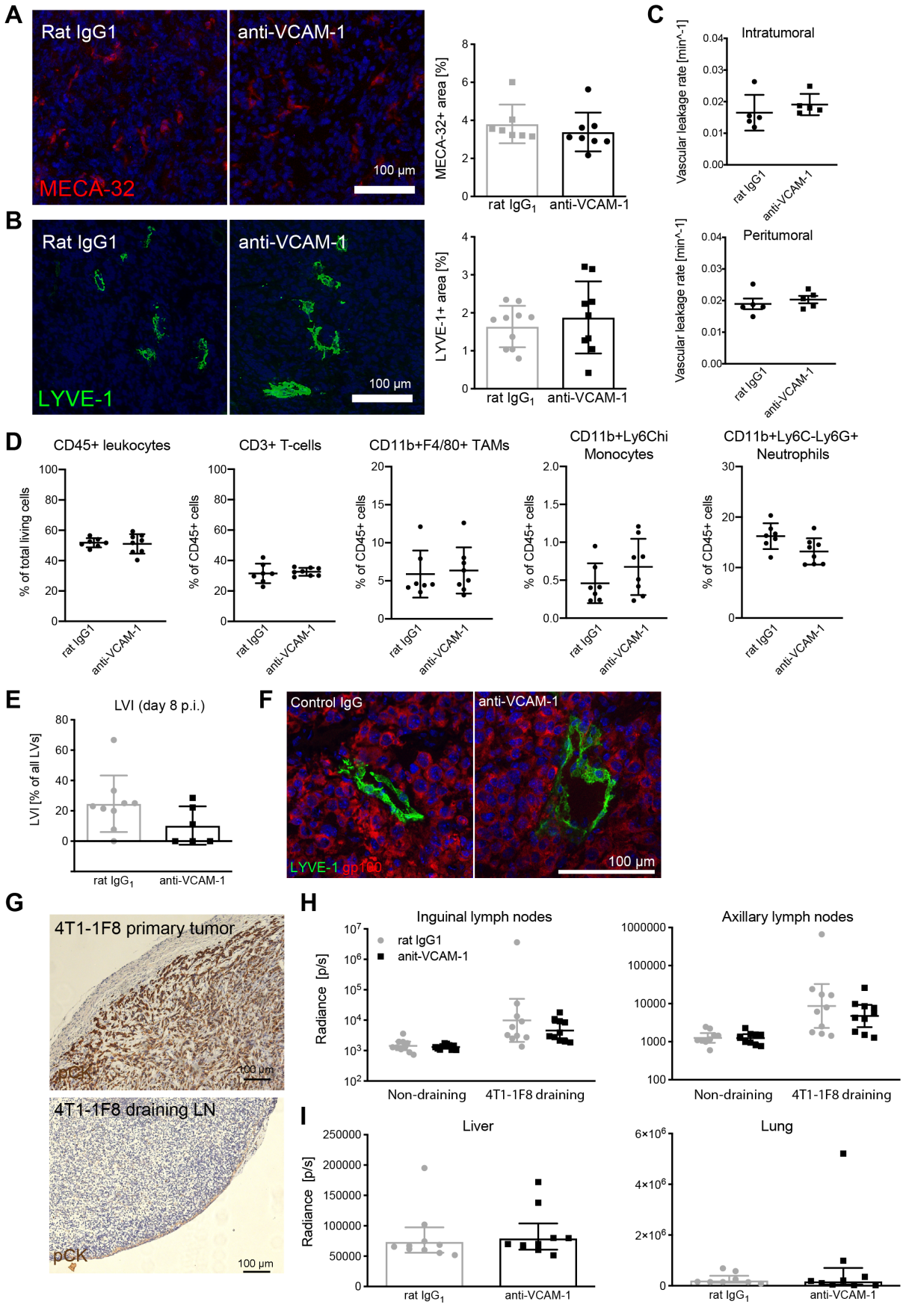

Figure S2: VCAM-1 inhibition has no influence on tumor angiogenesis, lymphangiogenesis and distant metastasis.

(A) Representative MECA-32 staining (red, left panels) and quantification (right panel) of the MECA-32$^+$ area in 4T1-1F8 tumors treated with control IgG or anti-VCAM-1 antibodies (N = 7 control / 8 anti-VCAM-1 treated tumors). (B) Representative LYVE-1 staining (green, left panels) and quantification (right panel) of the LYVE-1$^+$ area in 4T1-1F8 tumors treated with control IgG or anti-VCAM-1 antibodies (N = 10 control / 9 anti-VCAM-1 treated tumors). (C) Blood vessel permeability determined after i.v. injection of a near-infrared fluorescent tracer within the tumor (top panel) and in the peri-tumoral region (bottom panel) (N = 5 mice / group). (D) Flow cytometry analysis of tumor-infiltrating leukocyte subsets in 4T1-1F8 tumors treated with control IgG or anti-VCAM-1 antibodies (N = 7 control / 8 anti-VCAM-1 treated mice). (E) Quantification of the frequency of tumor cell-invaded lymphatic vessels at day 8 after implantation of 4T1-1F8 tumors (N = 8 control / 6 anti-VCAM-1 treated mice). Mice were treated with control IgG or anti-VCAM-1 every other day. (F) Representative immunofluorescence images of LYVE-1$^+$ lymphatic vessels in orthotopically implanted B16F10-VEGFC tumors treated with control IgG or anti-VCAM-1 antibodies. (G) Representative immunohistochemistry images showing homogenous pan-cytokeratin staining in primary 4T1-1F8 tumors (top panel), whereas no specific staining was detectable in draining LNs (bottom panel). (H) Endpoint (day 21) bioluminescence signal of inguinal (left panel) and axillary (right panel) LNs in 4T1-1F8 tumor bearing mice treated with control IgG or anti-VCAM-1 antibodies (N = 10 mice / group; bars represent geometric means + 95% CI). (I) Endpoint (day 21) bioluminescence signal of liver (left panel) and lung (right panel) in 4T1-1F8 tumor bearing mice treated with control IgG or anti-VCAM-1 antibodies (N = 10 mice / group; bars represent geometric means + 95% CI).

Supplementary Figure S3

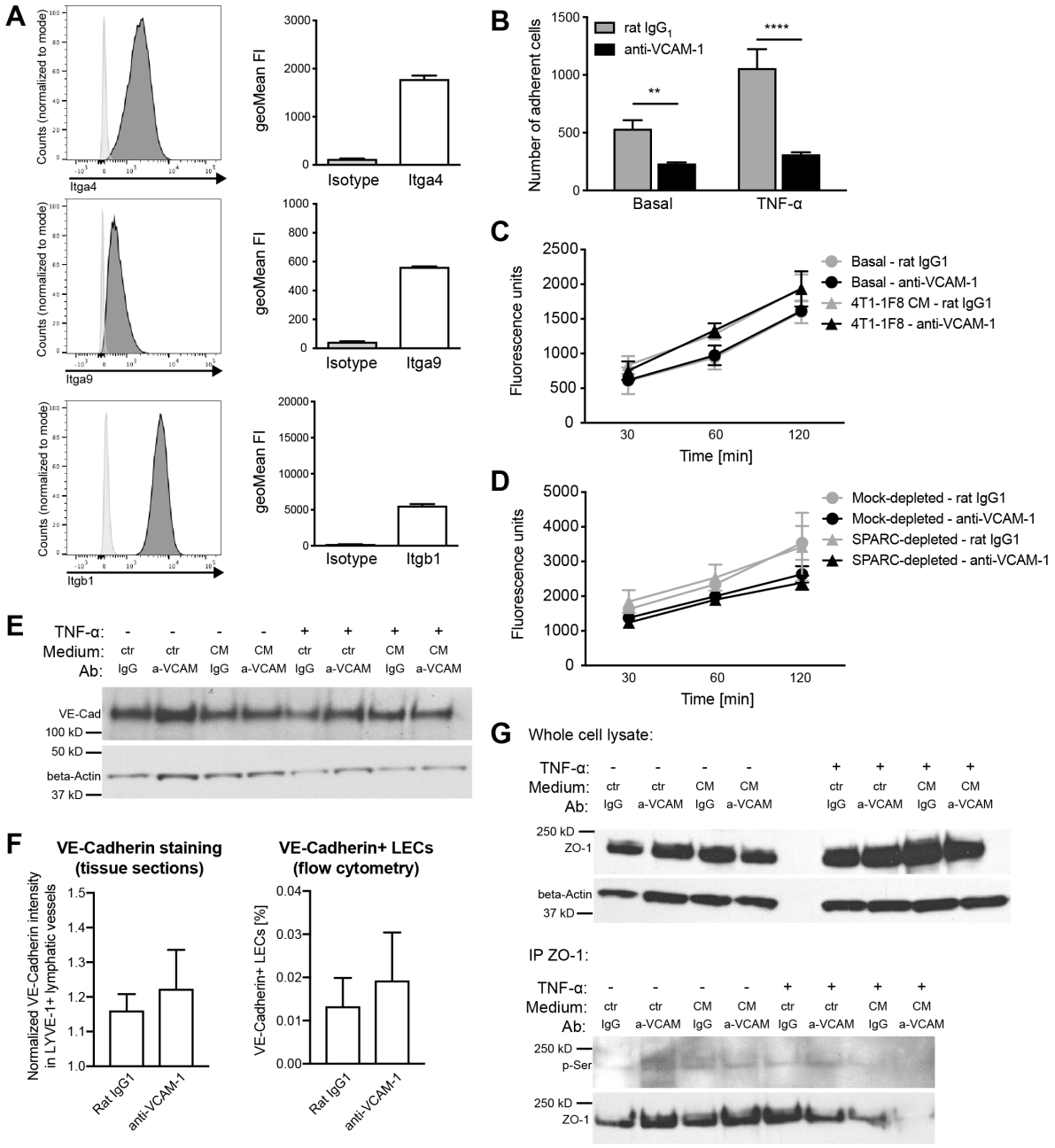

Figure S3: VCAM-1 blockade reduces B16F10 / LEC adhesion.
Representative FACS histograms (left panels) and staining quantification (right panels) of the classic VCAM-1 receptors integrin α4 (Itga4), integrin α9 (Itga9), and integrin β1 (Itgb1) in B16F10-VEGFC cells (N = 3). (B) Adhesion of fluorescently labelled B16F10-VEGFC cells to monolayers of cultured mouse LECs pre-treated with TNF-α or not and in presence of control IgG or VCAM-1 blocking antibodies (N = 3 wells / condition; 1 representative of 5 individual experiments is shown). (C) *In vitro* permeability of mouse LEC monolayers grown on transwell inserts (0.4 µm pore size) toward 70 kD FITC-dextran. LEC monolayers were left untreated overnight and were subsequently incubated with control or 4T1 CM in presence of control IgG or anti-VCAM-1 antibodies (N = 3 wells / condition; 1 representative of 3

individual experiments is shown). (D) *In vitro* permeability of mouse LEC monolayers grown on transwell inserts (0.4 μm pore size) towards 70 kD FITC-dextran. LEC monolayers were treated with TNF-α overnight and were subsequently incubated with 4T1 CM that was depleted of SPARC or not, in presence of control IgG or anti-VCAM-1 antibodies (N = 3 wells / condition; 1 representative of 3 individual experiments is shown). (E) Western blot of total VE-cadherin in cultured mouse LECs treated as indicated in Materials and Methods. One representative of two independent experiments is shown. ctr: control medium; CM: 4T1-1F8 conditioned medium; Ab: antibody; IgG: rat IgG_1; a-VCAM: anti-VCAM-1 (F) *Left panel:* VE-cadherin staining intensity within LYVE-1 lymphatic vessels was assessed by immunofluorescence staining of 4T1-1F8 tumor tissue sections and normalized to the overall staining intensity per image (= 1). *Right panel:* Frequency of VE-cadherin+ LECs in 4T1-1F8 tumors determined by flow cytometry. (G) *Top panel:* Western blot of total ZO-1 in cultured mouse LECs treated as in (E). One representative of two independent experiments is shown. *Bottom panel*: Immunoprecipitation of ZO-1 followed by immunoblotting for phospho-serine (p-Ser) and total ZO-1 (** $p < 0.01$; **** $p < 0.0001$).

SUPPLEMENTARY TABLES

Table S1:

RNAseq results, filtered for differentially expressed genes ($log_2FC > 2$, $FDR < 0.01$), including raw and normalized counts (TPM).